WISCONSIN

UC-20 f,g

UNIVERSITY OF WISCONSIN • MADISON, WISCONSIN

PLASMA PHYSICS

HIGH β STUDIES IN THE WISCONSIN TOROIDAL OCTUPOLE

J.H. Halle, A. Kellman, R.S. Post,
S.C. Prager, E.J. Strait, and M.C. Zarnstorff

DOE/ET53051/9 September 1980

UNIVERSITY OF WISCONSIN MADISON

NOTICE

Printed in the United States of America
Available from
National Technical Information Service
U.S. Department of Commerce
5285 Port Royal Road
Springfield, VA 22161

NTIS Price codes
Printed copy: A02
Microfiche copy: A01

HIGH β STUDIES IN THE WISCONSIN TOROIDAL OCTUPOLE

J.H. Halle, A. Kellman, R.S. Post,
S.C. Prager, E.J. Strait, and M.C. Zarnstorff

ABSTRACT

A wide range of MHD stable high β plasmas is produced in the Wisconsin Levitated Octupole. At or near the single fluid regime we obtain, in the bad curvature region, $\beta = nk(T_e+T_i)8\pi/B^2 \simeq 8\%$, twice the theoretical single fluid ballooning instability limit of 4%. We also obtain stable plasmas at $\beta \simeq 35\%$, 9 times the theoretical limit, in a regime in which both finite ion gyroradius and gyroviscosity effects are important.

The high β (= plasma pressure/magnetic pressure) magnetohydrodynamic ballooning instability is predicted to set a β limit for any average minimum B system such as tokamaks[1], tandem mirrors[2] and multipoles[3]. Ballooning mode study in a toroidal multipole is simplest in that multipoles may be operated without magnetic shear (unlike tokamaks) and contain an ignorable coordinate (unlike tandem mirrors). Thus high β multipole experiments can test ballooning mode theory; if multipole β limits are incorrectly predicted, present theory will be unreliable for other configurations. These β limits also influence the feasibility of a multipole advanced fuel reactor[4].

Extremely high β plasmas are produced[5] in the Wisconsin Levitated Toroidal Octupole in a search for ballooning effects. A broad range of MHD stable high β plasmas are obtained with parameters varying from the ideal single fluid to the kinetic regime. In all cases, β is evaluated locally in the bad curvature, high field region (Fig. 1). β is higher at nearly all other locations.

Near the single fluid regime we have attained $\beta = nk(T_e+T_i)8\pi/B^2$ of 8%, twice the theoretical single fluid ballooning limit of 4%. Since $L_p \sim 5\rho_i$, where $L_p = p/(\nabla p)$ is the pressure scale length and ρ_i is the ion thermal gyroradius, finite ion gyroradius effects should not be large. Twenty-five ion gyroradii are contained between the ring and wall. The electron-ion coulomb mean free path ($\sim$ 10 cm) is much smaller than the magnetic connection length ($\sim$ 100 cm), eliminating kinetic free streaming and particle trapping effects. The magnetic Reynolds number, S = resistive skin time/Alfven time, is about 500 implying that resistivity is ignorable. Since the predicted ballooning mode amplitude varies along a field line ($\underline{k}\cdot\underline{B}\neq 0$) and the field is shearless, resistive effects such as tearing and defeat of shear stabilization play no role.

To date, the highest β achieved, at lower magnetic field, is 35%, roughly 9 times the fluid stability limit. The plasma is MHD stable. For this plasma both finite ion gyroradius and viscous effects are important since $2\rho_i \sim L_p$ and the ordinary Reynolds number $R = V_A \ell \frac{\rho}{\mu} \lesssim 1$ where V_A, ℓ, ρ and μ are the Alfven speed, perpendicular scale length in the bad curvature region, mass density and ordinary viscosity, respectively. Although not a reactorlike regime, examination of these apparently strong stabilizing effects is of value to determine their role in the theory and if they can be simulated in a reactor. For this β = 35% case, the measured equilibrium diamagnetism also differs dramatically from the fluid prediction, probably due to ion gyroviscosity effects, as indicated below.

The hydrogen plasma is created by simultaneous, cross-field injection from two coaxial Marshall guns into the 1.4 m major radius toroid containing 4 levitated internal rings. $\beta \simeq 8\%$ is obtained, 400 μsec after injection, on the separatrix between the outer rings and wall (Fig. 1) with $n \simeq 5 \times 10^{13}$ cm^{-3}, $T_e \simeq T_i \simeq 15$ eV and a purely poloidal magnetic field of 860 G (30% of present capability). $\beta \simeq 35\%$ is obtained similarly with a magnetic field of 200 G and $n \simeq 2 \times 10^{13}$ cm^{-3}, $T_e \simeq T_i \simeq 9$ eV. Density is measured with a vertical path 70 GHz interferometer located at the midcylinder; this measures the separatrix density since most of its path is of constant density equal to the separatrix density. Density invariance along field lines is verified with Langmuir probes. Electron temperature is measured with a double Langmuir probe and ion temperature with a 1/4" diameter gridded electrostatic analyzer. T_e and T_i are equal, as expected, since the electron-ion equilibration time is ≈ 50 μsec. Edge neutral pressure is ≈ 10^{-5} torr.

Within 400 μsec after injection the plasma pressure becomes axisymmetric to within 20% and adopts a steady pressure profile peaked on the separatrix. Thereafter β decays with a 500 μsec time constant which is ≈ 1000 Alfven transit times, and roughly the classical diffusion time. No β related fluctuations or disturbances are observed in magnetic field, density or electrostatic potential.

The theoretical β limit for plasma stability to the ballooning mode is evaluated from linear single-fluid theory by numerically solving, in the Levitated Octupole geometry, the eigenvalue equation for marginal stability [5,6]:

$$\frac{\partial}{\partial \ell}\left(\frac{1}{\mu_o r^2 B}\frac{\partial X}{\partial \ell}\right) - p' \frac{D}{B} X = 0 \qquad (1)$$

where the fluid perturbation in the direction normal to a flux surface is $\xi_\psi = X/rB$, $p' = \partial p/\partial\psi$, ψ is the poloidal flux function, r is the major radius, ℓ is the direction parallel to B and $D = -2\,\mu_o/B^2(\partial/\partial\psi)(p+B^2/2\,\mu_o)$. The critical β for instability is obtained by finding the minimum p' for which a solution for $X(\ell)$ exists. The experimental pressure profile is used as input and the coefficients may be evaluated using either the vacuum magnetic field or the self-consistent equilibrium values calculated from numerical solution of the Grad-Shafranov equation[5]. The mode with even symmetry about the midplane (good curvature) region is the most unstable mode[5] with a threshold β value of 4%. The eigenfunction $X(\ell)$ peaks only gently in the bad curvature region. Greater localization requires large energy expenditure in field line bending.

The departure of the equilibrium magnetic field from its vacuum value has been measured and compared with the single fluid equilibrium code. In the region between a ring and the wall the theoretical plasma self-current ($\underline{\nabla P} \times \underline{B}/(B)^2$) reverses direction across the separatrix where the pressure peaks. Thus, the plasma displays regions of local diamagnetism ($\Delta B<0$) and local paramagnetism ($\Delta B>0$) as seen in Fig. 2[5]. For the $\beta \simeq 8\%$ plasmas at B = 860 G with 5 $\rho_i \sim L_p$, good agreement exists between experiment and fluid theory, in both magnitude and profile (Fig. 2). At the highest β ($\simeq 35\%$) case, in which 2 $\rho_i \sim L_p$ and viscosity effects are important, the measured field perturbation deviates from the single fluid expectation by a factor of 7 (Fig. 3). As the field is increased, gyroradius and viscosity effects decrease and the experimental ΔB is observed to approach the single fluid value (Fig. 3). However, even at the high fields the time behavior of β does not match that of $\Delta B/B$ which decays with a time constant of $\simeq$ 250 μsec. For the range of β considered, fluid theory predicts $\Delta B/B$ to be proportional to β; thus the fluid theoretical prediction for $\Delta B/(B\beta)$ is field independent.

To indicate the cause of the experimental deviation from the single fluid equilibrium two approaches are followed. In both cases only the region between the ring and wall is studied. The region is modelled by a one dimensional straight cylindrical plasma annulus bounded by 2 coaxial cylinders, the inner and outer ones representing a ring and the wall, respectively. This model accurately describes the corresponding Octupole region, as verified by comparing the analytical single fluid coax solution to the exact solution of the two dimensional Grad-Shafranov equation for the Octupole. The two results are nearly identical.

In the first approach a simple kinetic calculation allows gyroradii of any size by posing a Vlasov equilibrium distribution function dependent on constants of motion only; current is then directly computed. As an example, the annulus is filled with a spatially independent Maxwellian distribution function. Particles whose orbits intersect boundaries are eliminated. Numerical integration of the remaining distribution function, which still satisfies a Vlasov equilibrium, yields density and current density profiles. The current profiles are close to the single fluid prediction independent of the temperature, or average gyroradius, of the initial Maxwellian. Thus, large ion gyro-orbits can<u>not</u> in themselves account for the experimental results.

The second approach includes ion gyroviscosity through the two fluid equilibrium equations with the full pressure tensor[7,8]

$$nMv_{ir}v_{ir}' = neE_r - nev_{iz}B - p' - mn(v_{ir}-v_{er})\nu_{ei} + \frac{1}{r}\left\{\frac{2rp\tau}{1+4\omega^2\tau^2}\left[\frac{2}{3}(1+\omega^2\tau^2)v_{ir}' - \omega\tau v_{iz}'\right]\right\}' \qquad (2)$$

$$nMv_{ir}v_{iz}' = neE_z + nev_{ir}B - mn(v_{iz}-v_{ez})\nu_{ei} + \frac{1}{r}\left[\frac{2rp\tau}{1+4\omega^2\tau^2}\left(\frac{1}{2}v_{iz}' + \omega\tau v_{ir}'\right)\right]' \qquad (3)$$

$$nmv_{er}v'_{er} = -neE_r + nev_{ez}B - p' + mn(v_{ir}-v_{er})\nu_{ei} \quad (4)$$

$$nmv_{er}v'_{ez} = -neE_z - nev_{er}B + mn(v_{iz} - v_{ez})\nu_{ei} \quad (5)$$

where $' = \partial/\partial r$, and, v_{ir}, v_{er}, v_{iz}, v_{ez}, ω, τ are the ion and electron radial velocities, ion and electron axial velocities, ion cyclotron frequency and ion-ion collision time, respectively. The ion velocity differs from the single fluid value due to the viscous terms on the right side of equations (2) and (3). Viscous terms in the last two electron equations are absent since they are smaller by mass ratios. However, the electron velocity can deviate from its single fluid value since electrons collisionally couple to ions. In the $\beta \simeq 35\%$ plasmas, the viscous terms are of comparable magnitude to the other terms.

Assuming the magnitude of the radial velocities is roughly the collisional diffusion velocity, all terms containing v_{ir} and v_{er} are small (except near the edge where P becomes small). Thus we set $v_{ir} = v_{er} = 0$, permitting analytical solution for v_{iz}, v_{ez}, E_r and E_z. Employing these solutions, equations (2) and (4) combine to yield the axial (toroidal) current density, j,

$$jB = P' - C(\omega\tau)'$$

where C is an integration constant and P the total pressure. Thus the last term represents the desired deviation from single fluid theory. For proper choice of C, this term diminishes the current density

(Fig. 4) but maintains the overall shape, as observed experimentally. Detailed comparison with experiment awaits numerical solution of the full set of equations. Moreover, the theory is inaccurate in the highest β case where the gradient scale lengths are comparable to the mean free paths.

In summary, a range of MHD stable high β plasmas has been attained both in the kinetic regime with β = 35%, 9 times the fluid ballooning limit, and near the single fluid regime with β = 8%, twice the theorectical limit. Equilibrium measurements roughly agree with single fluid results in the latter case, but depart sharply in the former (kinetic) regime. The present experimental limit to β is a temporary limitation of the plasma sources.

We are grateful to S.V. Painchaud for performing the kinetic equilibrium calculation, to E.A. Rose for aid in the ion temperature measurement, to S. Garner for construction of the microwave interferometer, and to K.R. Symon, J.C. Sprott and J.D. Callen for many valuable suggestions.

This work was supported by U.S.D.O.E.

REFERNCES

1. D. Dobrott, D.B. Nelson, J.M. Greene, A.M. Glasser, M.S. Chance and E.A. Frieman, Phys. Rev. Letters 39, 943 (1977).

2. D.E. Baldwin, R.H. Cohen, T.A. Cutler, T.B Kaiser, B.G. Logan, Y. Matsuda, A.A. Mirin, L.D. Pearlstein, M. Parkolab, M.E. Rensink, T.D. Rognlien, 8th Int'l. Conf. on Plasma Physics and Controlled Fusion Research, IAEA (1980).

3. T. Ohkawa and D.W. Kerst. Nuovo Cim. 22, 784 (1961).

4. R.W. Conn, D. Arnush, J. Dawson, D.W. Kerst, V. Vanek in Fusion Reactor Design Concepts, IAEA, Vienna, 721 (1978).

5. S.C. Prager, J.H. Halle, M.W. Phillips, R.S. Post and J.C. Twichell, Nuclear Fusion, 20, 635 (1980).

6. J.L. Johnson, R.M. Kulsrud, K.E. Weiner, Plasma Phys. 11, 463 (1979).

7. S. Chapman, T.G. Cowling, The Mathematical Theory of Nonuniform Gases, Cambridge University Press, Cambridge (1961).

8. S. Braginskii, Zh. Eksp. Teor. Fiz. 33 459 (1957) [Sov. Phys. JETP 6, 366 (1958)]

FIGURE CAPTIONS

Fig. 1: Poloidal magnetic flux plot of the Levitated Octupole, indicating bad curvature region where β is evaluated. Plasma pressure peaks on the separatrix (dashed line). Major radius = 1.4 meters.

Fig. 2: Single fluid theoretical and experimental spatial profile (between outer ring and wall) of perturbation, ΔB, to the poloidal magnetic field due to the equilibrium diamagnetic currents for $\beta \simeq 8\%$. Plasma pressure peaks at the separatrix (Sep). Experimental error $\simeq$ 25% from shot to shot variations.

Fig. 3: Theoretical and experimental fractional change in the magnetic field (at the separatrix in the bad curvature region) due to plasma diamagnetic curents versus poloidal magnetic strength. $\Delta B/B$ is normalized to the separatrix β value so that single fluid theory yields a horizontal line.

Fig. 4: Spatial profile of the equilibrium current density for the coaxial model of the Octupole from ideal single fluid theory and two fluid theory including viscous terms in the pressure tensor. The two fluid theory is not plotted near the boundary region where the method of solution breaks down. A gaussian pressure profile is assumed.

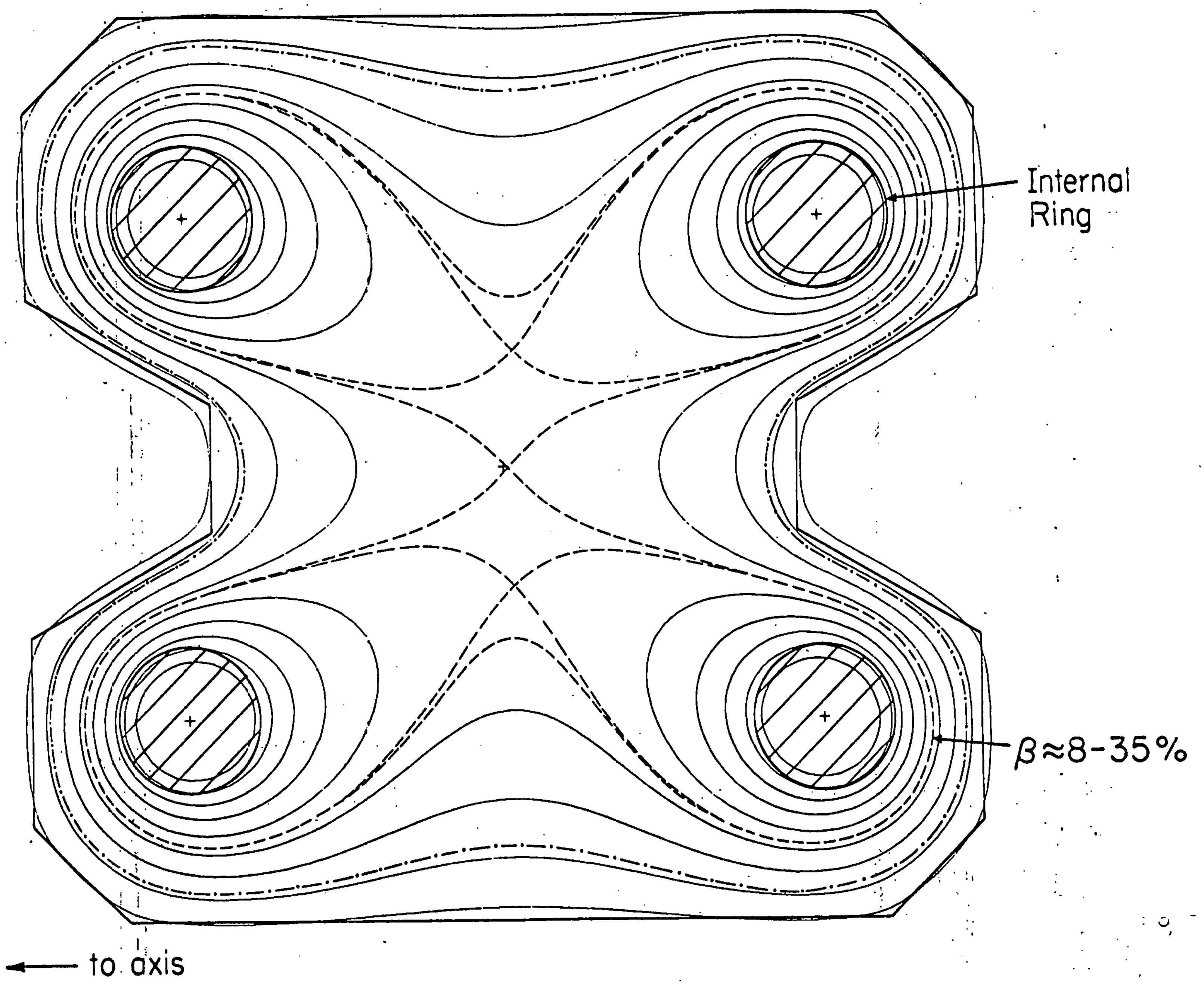

FIG. 1

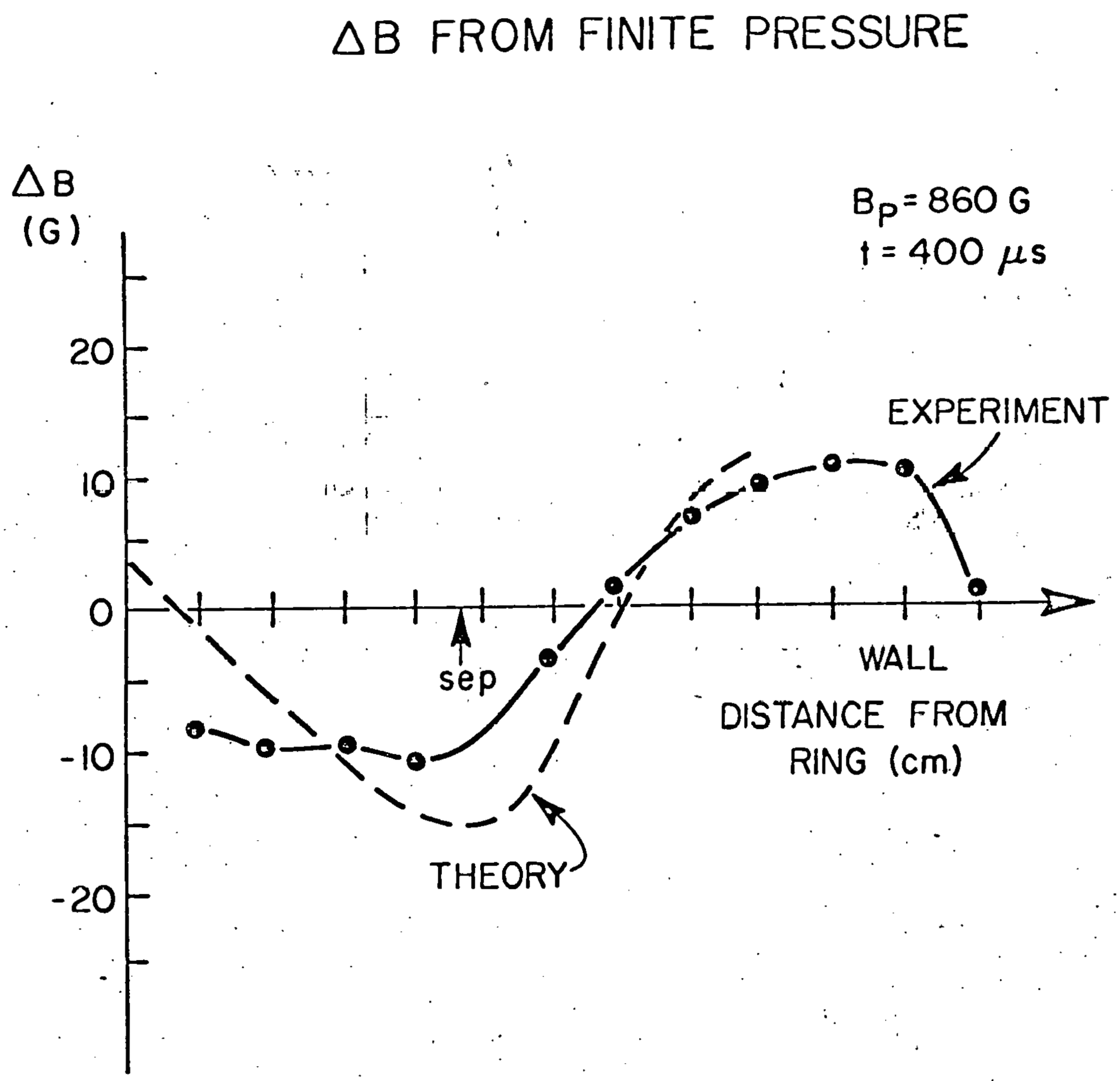
ΔB FROM FINITE PRESSURE
ΔB
(G)
B_P = 860 G
t = 400 μs
20
10
0
-10
-20
EXPERIMENT
sep
WALL
DISTANCE FROM
RING (cm)
THEORY

FIG. 2

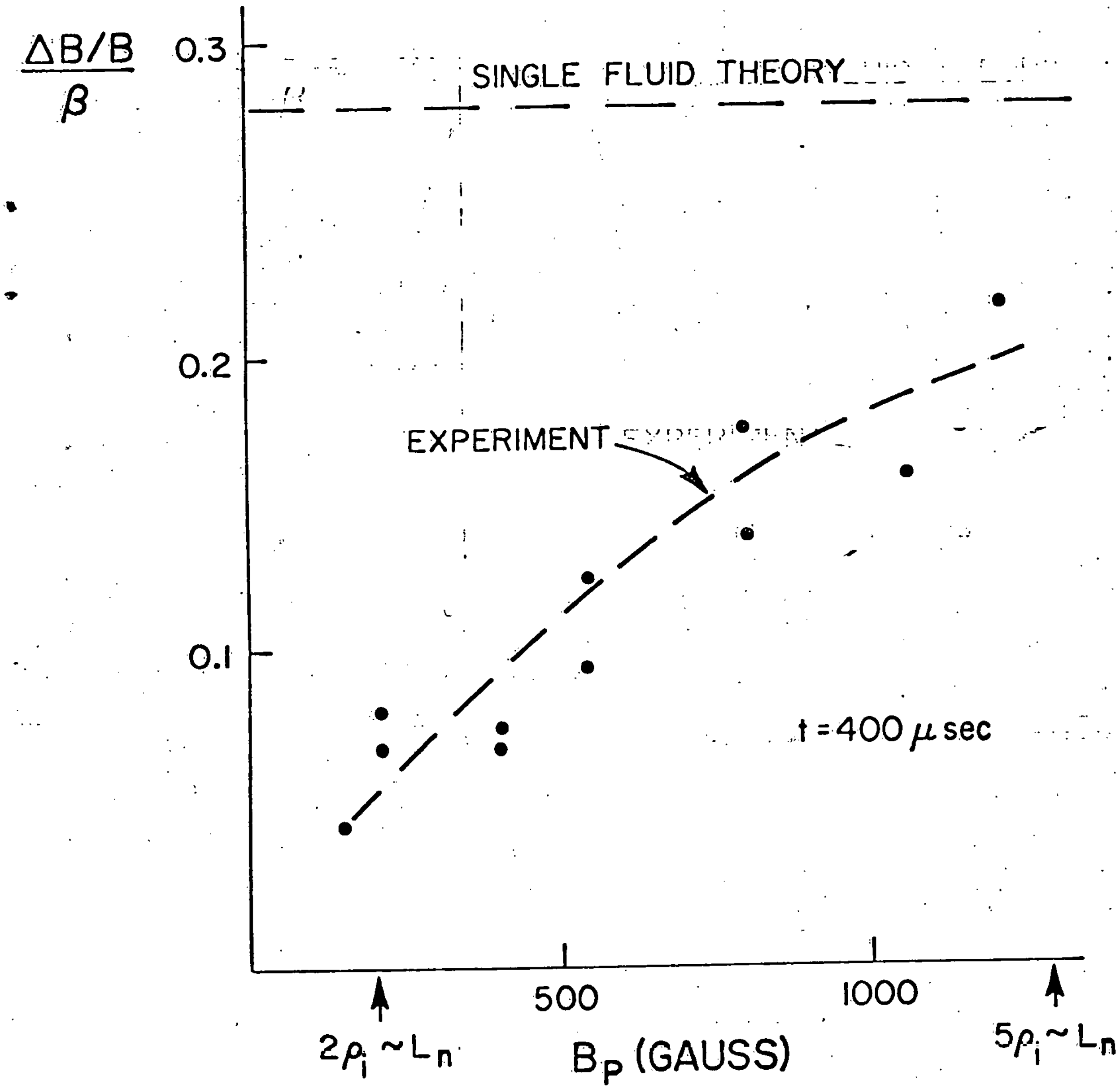

ΔB/B
β
0.3
0.2
0.1
SINGLE FLUID THEORY
EXPERIMENT
t = 400 μ sec
500
1000
2ρi ~ Ln
BP (GAUSS)
5ρi ~ Ln

FIG. 3

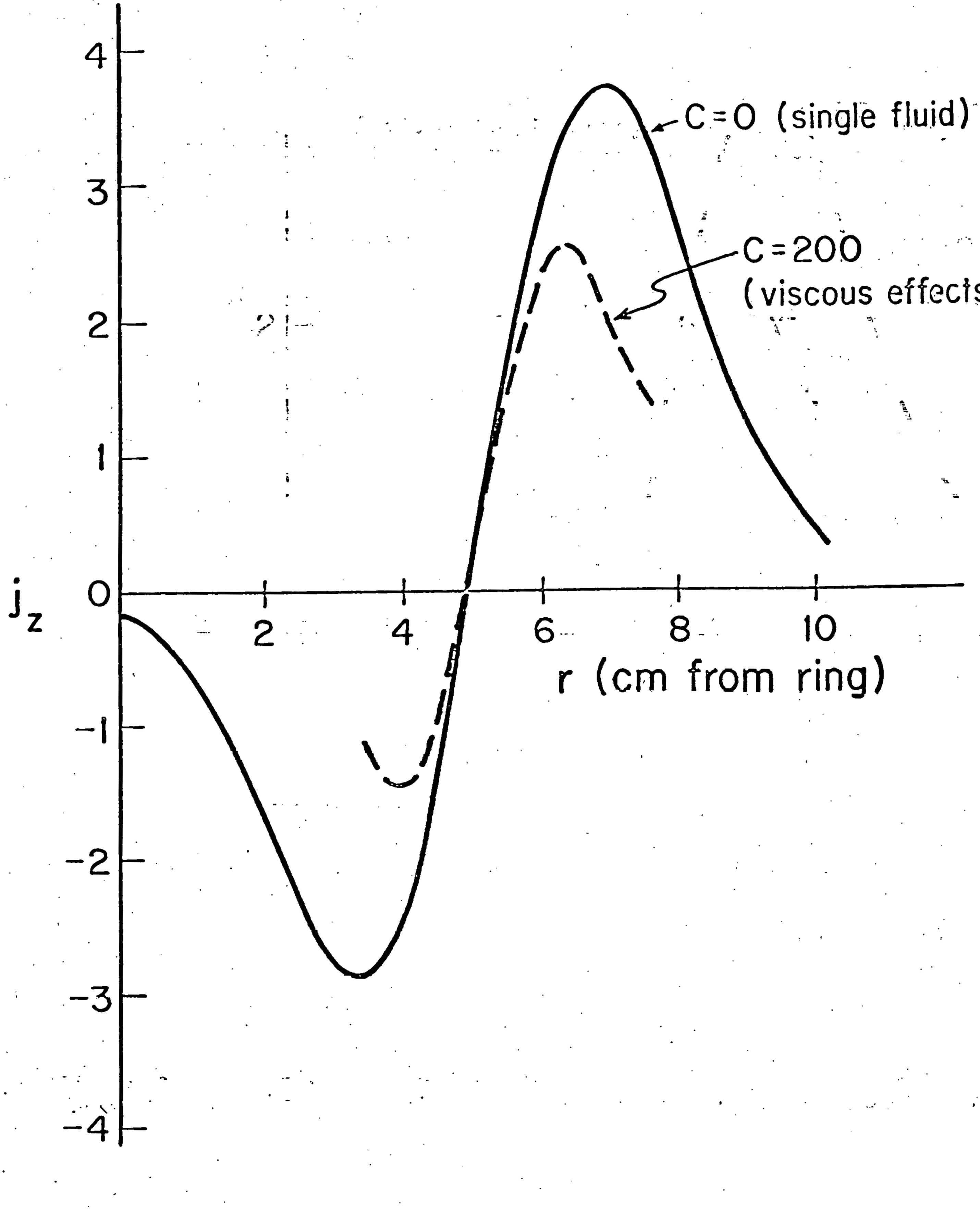

4
3
2
1
0
-1
-2
-3
-4
j_z
2
4
6
8
10
r (cm from ring)
C=0 (single fluid)
C=200
(viscous effects)

FIG. 4

EXTERNAL DISTRIBUTION IN ADDITION TO UC-20

R.W. Conn, University of California, Los Angeles
J.W. Flowers, University of Florida
H.S. Robertson, University of Miami, FL
E.G. Harris, University of Tennessee
M. Kristiansen, Texas Technical University
Plasma Research Laboratory, Australian National University
P.E. Vandplas, Association Euratom-Etat Belge, Belgium
P. Sananaka, Institute de Fisica-Unicamp, Brazil
A.M. Dupas, C.E.N.G., Dph-PFG-SIG, France
M.A. Loyau, Centre d'Etudes Nucleaires, France
G. VonGierke, Max-Planck-Institut Für Plasma Physic, Germany
R. Toschi, Associazione Euratom-Cnen Sulla Fusion, Cento Gas Ionizzati, Italy
K. Takayma, IPP Nagoy Imoversotu, Japan
K. Uo, Kyote University, Japan
K. Yamanto, JAERI, Japan
B. Lehnert, Royal Institute of Technology, Sweden
E.S. Weibel, CRPP, Ecole Polytechnique Federale de Lausanne, Switzerland
A. Gibson, Culham Laboratory, UK
R.S. Pease, Culham Laboratory, UK
D.R. Sweetman, Culham Laboratory, UK
J.B. Taylor, Culham Laboratory, UK
M.H. Hellberg, University of Natal, Durban, South Africa
Cheng-chung Yang, Chinese Academy of Sciences, Lanchow, Peoples Republic of China
Chi-shis Li, Chinese Academy of Sciences, Peking, Peoples Republic of China
Hsiao-wu Chêng, Chinese Academy of Sciences, Shanghai, Peoples Republic of China
Yi-chung Cho, Chinese Academy of Sciences, Peking, Peoples Republic of China
Fu-chia Yang, Futan University, Peoples Republic of China
Mei-ling Yeh, Chinese Academy of Sciences, Lanchow, Peoples Republic of China
Wei-chung Change, Chinese Academy of Sciences, Shanghai, Peoples Republic of China
Kuei-wu Wang, Chinese Academy of Sciences, Loshan County, Peoples Republic of China
Chûn-hsien Chên, Chinese Academy of Sciences, Peking, Peoples Republic of China
Li-tsien Chiu, Chinese Academy of Sciences, Peking, Peoples Republic of China
Miao-sun Chen, Chinese Academy of Sciences, Peking, Peoples Republic of China

6 for Chicago Operations Office
10 for individuals in Washington Offices

INTERNAL DISTRIBUTION IN ADDITION TO UC-20

100 for local group and file